ACHIEVEMENT OF SMALL BEAM SIZE AT ATF2 BEAMLINE

T. Okugi†, KEK/SOKENDAI, Tsukuba, Ibaraki, Japan
ATF International Collaboration

Abstract

The purpose of ATF2 project is to develop and establish a new final focus method, called "Local Chromaticity Correction (LCC)", which will be used at International Linear Collider (ILC). ATF2 project has been performed by utilizing a small emittance beam of KEK Accelerator Test Facility (KEK-ATF). The beam optics of ATF2 is designed to be based on the same method as ILC, with the equivalent beam energy spread and natural chromaticity, the tolerances of magnetic field errors are also equivalent to the ILC final focus system. The vertical beam size was focused to less than 41 nm at the bunch population of 0.7×10^9 at ATF2 virtual IP. The achieved beam size is close to the ATF2 target value of 37 nm. The bunch population at the recent ATF2 beam operation is much smaller than ILC. The reason why the bunch population of ATF2 is smaller than ILC is strong intensity dependence of vertical beam size at the virtual IP. The candidate of the intensity dependence source is IP angle jitter via wakefield.

INTRODUCTION

The KEK-ATF [1, 2, 3, 4] has been built for accelerator R&D, especially for ILC [5]. Figure 1 shows a schematic view of the KEK-ATF accelerator complex. KEK-ATF consists of an injector linac, a damping ring, a beam extraction line and ATF2 beamline. The purpose of the damping ring is to supply a low emittance beam to the extraction line and ATF2 beamline for accelerator R&D. The vertical beam emittance produced by damping ring is less than 10 pm [6, 7] (smaller than 12 pm of the ATF2 requirement). The corresponding 30 nm normalized emittance is comparable with the requirement of the ILC beam delivery system. The ATF2 beamline was constructed to study the ILC final focus system, utilizing the small emittance beam generated by the damping ring.

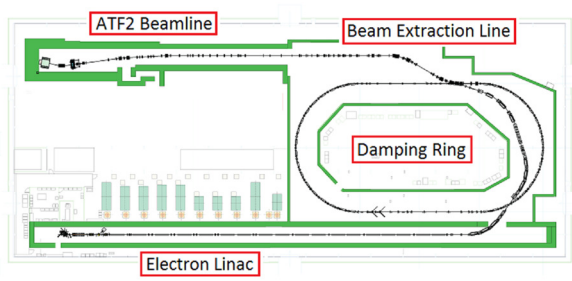

Figure 1: Accelerator complex of KEK-ATF, consisting of an electron linac, a damping ring, a beam extraction line and the ATF2 beamline.

Table 1: Beam and Optics Parameters for the ILC and ATF2 Final Focus Beamlines (10 × 1 Optics)

	ILC	ATF2
E [GeV]	250	1.28
L^* [m]	4.1	1.0
ε_x [nm] / ε_y [pm]	0.02 / 0.07	2 / 12
$\gamma\varepsilon_x$ [μm] / $\gamma\varepsilon_y$ [μm]	10 / 0.035	5 / 0.030
β_x^* [mm] /β_y^* [mm]	11 / 0.48	40 / 0.10
σ_x^* [μm] /σ_y^* [nm]	0.47 / 5.9	8.9 / 37
σ_z [mm]	0.3	7.0
σ_p/p	0.12 %	0.07%

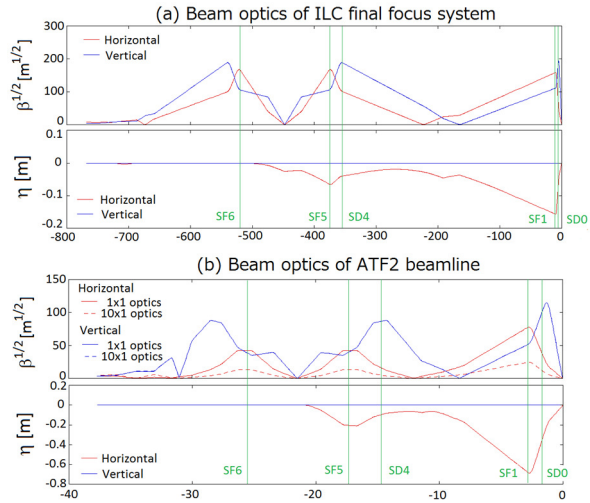

Figure 2: Beam optics of the ILC final focus beamline (a) and the ATF2 beamline (b). Both the 1×1 optics and the 10×1 optics are shown.

ATF2 BEAMLINE

Beam Optics of ATF2 Beamline

The ILC final focus system is designed based on the LCC technique [8]. The main purpose of the ATF2 beamline is to demonstrate beam focusing with the LCC method, and to establish a beam tuning method for ILC final focus systems. Therefore, the ATF2 beam optics was designed based on the LCC scheme. The IP horizontal and vertical beta-functions (β_x^*, β_y^*) of ATF2 were originally designed to generate the same horizontal and vertical chromaticities as ILC (1×1 optics). However, since the ATF2 beam energy is much smaller than ILC, the geometrical aberrations of ATF2 are much larger than ILC, and the effect of the multipole errors are larger than ILC. Therefore, in recent ATF2 beam operation, the ATF2 beamline was operated with a 10 times larger horizontal IP beta-function than that of original optics in order to reduce sensitivity to the multipole errors. We call the beam optics as "10×1 optics". The beam optics for ILC and ATF2 beamlines are shown in Fig. 2, and the main parameters are listed in Table 1. The

† toshiyuki.okugi@kek.jp

ISBN 978-3-95450-169-4

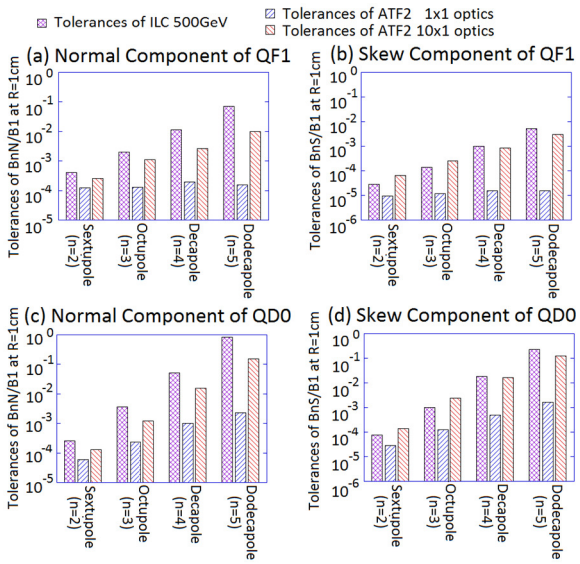

Figure 3: Tolerances of multipole field errors for the final doublet (QF1 and QD0) of the ILC and ATF2 final focus beamlines.

multipole field error tolerances of IP vertical beam size for ILC and ATF2 final doublet (QF1, QD0) are shown in Fig. 3. The tolerances are defined as the error which induce a 2% of IP vertical beam size growth. Figure 3 shows the tolerances of the multipole field errors in ATF2 10×1 optics are comparable with those of ILC.

Beam Size Monitor

A nanometer scale beam size monitor [9] was demonstrated at SLAC FFTB, measuring a beam size of approximately 70 nm [10]. This IP beam size monitor (IP-BSM) used at FFTB was modified and installed at the ATF2 virtual IP. The IP-BSM uses a fringe pattern formed by two interfering laser beams. The laser fringe pitch is defined by the wavelength (λ) and crossing angle of the two laser paths (θ) as $\mathrm{d} = \lambda/2\sin(\theta/2)$. Compton scattered photons from the transverse overlap of the laser fringe pattern with the beam are measured downstream of the IP. When the laser fringe phase is scanned, the Compton scattered signal is modulated with the fringe phase. The modulation depth (M) can be defined by using the maximum and minimum Compton signals (N_{max}, N_{min}) as $M = (N_{max} - N_{min})/(N_{max} + N_{min})$. The IP beam size is evaluated as a function of the modulation depth:

$$\sigma_y = \frac{1}{k_y}\sqrt{\frac{1}{2}\ln\left(\frac{C\,|\cos\theta|}{M}\right)} \quad , \; k_y = \frac{\pi}{d} \; , \qquad (1)$$

where C expresses the contrast reduction of the laser fringe pattern. Reduction of the laser fringe contrast is caused by deteriorated laser spatial coherency, mismatch in the overlap of the two laser beams *etc.*.

Equation (1) shows the measuring range of the beam size measurement depends on the laser fringe pitch. The laser wavelength used in the ATF2 IP-BSM was changed from 1064 nm to 532 nm to measure the smaller beam size, and 3 laser crossing modes (2-8° mode, 30° mode, 174° mode) were prepared to extend the dynamic range of the beam size measurements [11].

Linear Optics Tuning Procedure

There are 5 sextupoles in the ATF2 beamline, as in the ILC final focus beamline (see Fig. 2). The transverse positions of all the sextupoles are controlled using magnet movers. When a sextupole is moved horizontally, a quadrupole field is generated. The strength of the generated quadrupole field is proportional to the horizontal offset and changes the horizontal and vertical beam waists (α_x and α_y), IP horizontal dispersion η_x and its derivative η_x'. The linear optics tuning knobs of AX, AY, EX and EPX knobs are calculated as orthogonal sets of horizontal offsets of the sextupoles, only individually changing the linear knob components α_x, α_y, η_x and η_x', respectively [12].

When a sextupole is moved vertically, a skew quadrupole field is generated. The strength of the generated skew quadrupole field is proportional to the vertical offset and changes the vertical dispersion η_y, the derivative η_y' and xy coupling components at the virtual IP, especially $\langle x'y\rangle$. The linear optics tuning knobs of EY, EPY and COUP2 knobs are calculated as orthogonal sets of the vertical offsets of the sextupoles, only individually changing the η_y, η_y' and $\langle x'y\rangle$, respectively.

The IP vertical beam size is sensitive to the beam waist offset (AY), the virtual IP vertical dispersion (EY) and the amount of xy coupling at the IP (COUP2). These linear knobs are used for IP vertical beam size tuning during ATF2 beam operations. The IP vertical beam size can be expressed as:

$$\sigma_y^2 = \varepsilon_y\beta_y^* + \Delta\sigma_{y,MP}^2 + (\sigma_{AY} + \mathrm{AY})^2 + (\sigma_{EY} + \mathrm{EY})^2 + (\sigma_{XY} + \mathrm{COUP2})^2, \qquad (2)$$

$$\sigma_{AY} = \sqrt{\frac{\varepsilon_y}{\beta_y^*}}W_y \; , \quad \sigma_{EY} = \eta_y\frac{\sigma_p}{p} \; , \quad \sigma_{XY} = \sqrt{\frac{\beta_x}{\varepsilon_x}}\langle x'y\rangle \; ,$$

where W_y is the vertical beam waist offset, and $\Delta\sigma_{y,MP}$ is the IP beam size contribution due to multipole field errors. Inserting Eq. (2) into Eq. (1), the modulation depth can be expanded as:

$$\begin{aligned} M = C\,|\cos\theta|\,&\exp\{-2k_y^2(\varepsilon_y\beta_y^* + \Delta\sigma_{y,MP}^2)\} \\ &\times \exp\{-2k_y^2(\sigma_{AY} + \mathrm{AY})^2\} \\ &\times \exp\{-2k_y^2(\sigma_{EY} + \mathrm{EY})^2\} \\ &\times \exp\{-2k_y^2(\sigma_{XY} + \mathrm{COUP2})^2\} \quad . \end{aligned} \qquad (3)$$

The 1st line of Eq. (3) is the maximum amplitude of the modulation depth, corresponding to the minimum achievable beam size after application of the linear knob corrections. The 2nd to 4th lines of Eq. (3) are the responses of the linear knobs. Since the modulation depth exhibits a Gaussian response to the linear knobs, the optimum setting of a linear knob corresponds to the peak of the fitted Gaussian function.

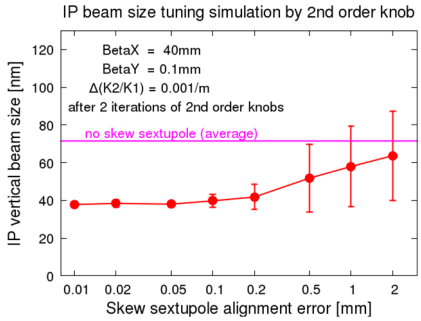

Figure 4: IP beam size simulation after 2nd order knobs. Horizontal axis is the initial alignment errors of skew sextupoles.

2nd Order Optics Tuning Procedure

Second order aberrations can be generated, for example, when there are sextupole field errors present in any magnets. There are 5 normal sextupoles in the ATF2 final focus beamline (see Fig. 2). The strengths of the sextupoles in the final focus beamline are set for cancelling chromatic and geometrical aberrations. On the other hand, the number of parameters that affect the horizontal and vertical beam size growth at the virtual IP is six (T_{122}, T_{126}, T_{166}, T_{144}, T_{324} and T_{346}). Therefore, T_{144} is ignored to make the ATF2 IP beam size tuning knobs because the effect of T_{144} is expected to be insignificant. Tuning knobs of X_{22}, X_{26}, X_{66}, Y_{24} and Y_{46} are calculated as orthogonal sets of strength changes of 5 sextupoles, which change only the components (T_{122}, T_{126}, T_{166}, T_{324} and T_{346}), respectively.

Furthermore, we installed 4 skew sextupoles (SK1-SK4) into the beamline to correct the 2nd order vertical optics errors at the virtual IP (T_{322}, T_{326}, T_{366} and T_{344}). The tuning knobs (Y_{22}, Y_{26}, Y_{66} and Y_{44}) to correct the skew sextupole field error components (T_{322}, T_{326}, T_{366} and T_{344}) are calculated as orthogonal sets of strength changes of 4 sextupoles, which change only the components. Since the 2nd order errors T_{322}, T_{326}, T_{366} and T_{344} could only be corrected only by using skew sextupoles, the skew sextupoles are important for IP beam size tuning in ATF2. Since the modulation depth exhibits a Gaussian response to the 2nd order knobs like linear knobs, the optimum setting of a 2nd order knob corresponds to the peak of the fitted Gaussian function.

The linear and 2nd order optics tuning for ILC IP is designed as the same procedures for ATF2 beam size tuning at the virtual IP.

IP BEAM SIZE OF ATF2 VIRTUAL IP

Beam Tuning Recipe of ATF2 IP Tuning

A nominal ATF2 beam tuning procedure is explained in this section. At the beginning of ATF2 beamline tuning, all of the sextupoles are turned off. Then, the orbit tuning is carried out. The corrected beam orbit is kept by using an orbit drift feedback. Since the vertical beta-function is reached up to approximately 10,000 m in ATF2 beamline,

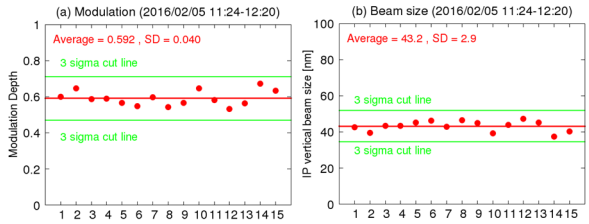

Figure 5: IP-BSM modulation and the beam size after the IP beam size tuning in 2016 February. The beam size was evaluated as $C = 1$ in Eq. (1).

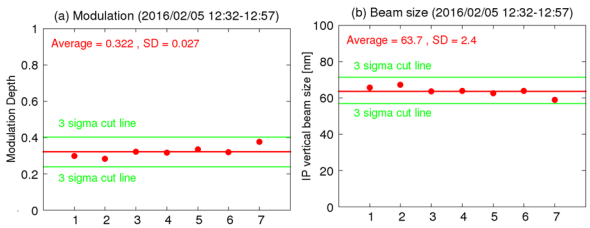

Figure 6: IP-BSM modulation and the beam size without skew sextupoles (just after the measurement of Fig. 5). The beam size was evaluated as $C = 1$ in Eq. (1).

the feedback corrector must be controlled within the accuracy of 0.01 Gauss · m. Therefore, the air core correctors are used for the orbit feedback. After the orbit tuning, the IP horizontal and vertical beam divergences are set to the design values. The beam waists are also set to the ATF2 virtual IP.

The magnetic centres of the sextupoles must be aligned with respect to the corrected beam orbit in order to avoid the linear optics deformation by the sextupoles. The offsets are measured by BBA techniques. It is very important to tune the beam orbit to magnetic centres of sextupoles in ATF2 beamline tuning. Figure 4 shows the IP beam size simulation to explain the importance of the magnetic centre alignment. The $k_2/k_1 = 10^{-3}\mathrm{m}^{-1}$ at $r = 1$ cm of sextupole field errors were assumed to all ATF2 quadrupoles, and the position of skew sextupoles were misaligned as initial condition. Then, the IP beam size was minimized by using 2nd order knobs in simulation. Simulation results show that the skew sextupoles must be aligned within 100 μm accuracies in order to make 2nd order knobs effective.

The sextupoles are turned on after the magnetic centre positions are moved with respect to the beam orbit. Then, the IP beam size is minimized by using the linear and 2nd order knobs.

Result of IP Beam Size Tuning

Figure 5 shows the IP-BSM modulation in February 2016. The beam tuning was followed by the tuning procedure of the previous section. Two iterations of 2nd order knob tuning (Y24, Y46, Y22, Y26, Y66 and Y44) were applied to minimize the IP vertical beam size. The linear knob tuning was also carried out in between each set of 2nd order knob tunings. The average modulation of 15 measurements was 0.592, and it corresponds to 43.2 nm vertical beam size

ISBN 978-3-95450-169-4

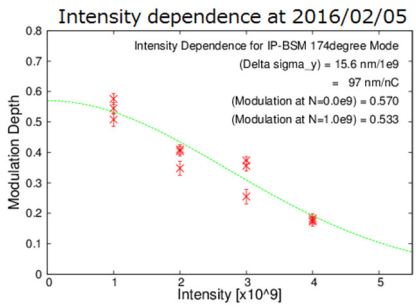

Figure 7: Typical intensity dependence of the vertical beam size at ATF2 virtual IP.

for $C = 1$ in Eq. (1). The bunch population was $N = 1 \times 10^9$.The IP-BSM modulation without skew sextupoles was also measured just after the measurement of Fig. 5. Results are shown in Fig. 6. The average beam size was increased to be 63.7 nm. It shows the skew sextupole field to correct the 2nd order optics errors of T_{322}, T_{326}, T_{366} and T_{344} were effective to focus the beam at ATF2 virtual IP.

The highest modulation at ATF2 virtual IP is 0.622, and it corresponds to 41.1 nm vertical beam size for $C = 1$ in Eq. (1). The modulation was measured at $N = 0.7 \times 10^9$ in March 2016 after the beam jitter subtraction with FONT feedback [13, 14]. The achieved beam size is close to the ATF2 target value of 37 nm.

INTENSITY DEPENDENCE

Present Situation of Intensity Dependence

The typical bunch population is $N = 1 \times 10^9$ for the beam size measurement at ATF2 virtual IP. It is 20 times smaller than ILC. The reason why the IP beam size was measured at the low intensity is its strong intensity dependence [15]. Figure 7 shows the typical intensity dependence

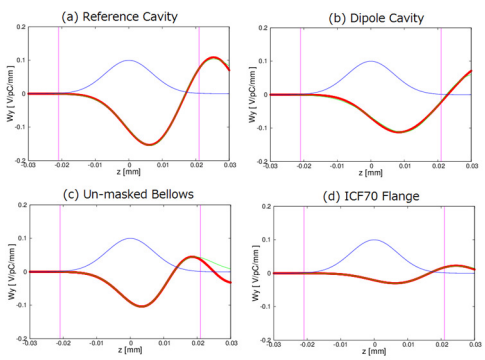

Figure 8: wake potentials for the electron beam with the bunch length of $\sigma_z = 7$ mm.

Table 2: Number of Components in ATF2 Beamline

Component	Number
C-band reference cavity	2
C-band dipole cavity	23
Un-masked bellows	11
ICF70 flange	87

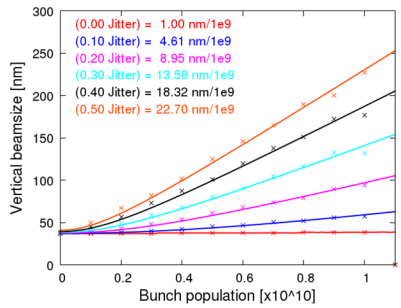

Figure 9: Simulation results of the ATF2 intensity dependences. In the simulation, the wake potentials are assumed for $\sigma_z = 7$ mm.

of ATF2 vertical beam size. The typical intensity dependence is $\Delta\sigma_y^*/N = 15\,\mathrm{nm}/10^9$electrons. The strong intensity dependence restricts the beam size measurement at higher bunch charge.

Candidate of the Intensity Dependence Source

The candidate of the source of the intensity dependence is a beam angle jitter via wakefield. The typical vertical beam size of ATF2 final focus beamline is 300-400 μm, and the beam jitter is 20-40 % of the beam size. Furthermore, since the phase advances to ATF2 virtual IP are separated by 90° from wakefield sources, the orbit kicks result the position changes at the virtual IP. Therefore, the beam position jitters at wakefield sources generate the IP position jitter. Since the IP-BSM measures the beam size by accumulating a lot of laser-beam collisions, the IP position jitter makes the evaluated IP beam size bigger. Furthermore, the kick angle by the wakefield is different along the longitudinal position, the wakefield also generates the beam size growth within the bunch.

The intensity dependence by the IP angle jitter via wakefield were simulated. The bunch length of electron beam was assumed to 7 mm. The wake potentials of ATF2 vacuum components were evaluated [16], and the wake potentials for an electron beam with the bunch length of $\sigma_z = 7$ mm were shown in Fig. 8. The number of components in ATF2 beamline are listed in Table 2. The simulation results [17] of the ATF2 intensity dependences are shown in Fig. 9. The simulation says typical intensity dependence on the ATF2 virtual IP beam size may be explained by 30-40 % of the IP angle jitter. The comparative study of the intensity dependence will be planned in 2016 autumn beam operation by reducing the amount of wakefield sources in ATF2 beamline.

The Effect of Angle Jitter via Wakefield for ILC

Since the ILC beam energy is 2 order larger than that of ATF2, the beam size and the beam jitter in the final focus beamline is much smaller than ATF2. The kick angle by wakefield is also much smaller than ATF2. Furthermore, since the bunch length of ILC is also much different from ATF2 (Table 1), the kick voltages of ILC and ATF2 are different even when the wakefield sources are same. ATF2

uses a lot of cavity BPMs, and ILC is also designed to use a lot of cavity BPMs. The dipole cavities are major wakefield sources in ATF2 beamline. The position change by IP angle jitter is roughly proportional to the sum of the beta functions at the dipole cavities as $\Delta y_{IP}/\sigma_y^* \propto NW\sum\beta_y$. The wake potentials of the ATF2 dipole cavity W for $\sigma_Z = 0.3$ mm (ILC beam) and $\sigma_Z = 7.0$ mm (ATF2 beam) are shown in Fig. 10. The IP angle jitter dependence by the dipole cavities at $N = 1 \times 10^9$ is shown in Fig. 11. The kick angle for $\sigma_Z = 0.3$ mm is approximately 40 % of that for $\sigma_Z = 7.0$ mm. The effects of the ATF2 and ILC intensity dependence effects by the IP angle jitter via wakefield are summarized in Table 3. The effect of ILC is 22% of ATF2 even if the bunch population is 20 times larger than ATF2. Therefore, we can consider that the effect is insignificant for ILC, though the strong intensity dependence of ATF2 is generated by the IP angle jitter via wakefield.

SUMMARY

The ATF2 beam optics was designed based on the LCC scheme of ILC. In ATF2 originally designed optics, the IP horizontal and vertical beta-functions were designed to generate the same horizontal and vertical chromaticities as ILC. However, since the ATF2 beam energy is much smaller than ILC, the ATF2 beamline was operated with a 10 times larger horizontal IP beta-function than the original optics in order to reduce sensitivity to the multipole errors in recent ATF2 beam operation. The effect of the multipole field errors for the recent ATF2 beam optics were comparable with the design for ILC IP vertical beam size tuning.

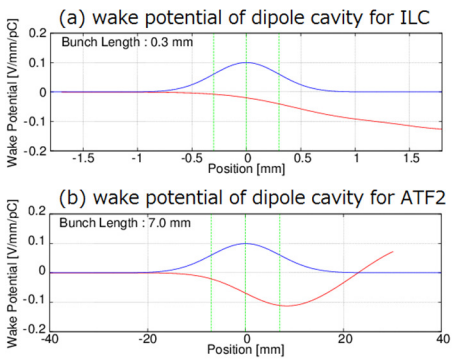

Figure 10: Wake potentials of ATF2 dipole cavity. (a) $\sigma_Z = 0.3$ mm (ILC bunch length), (b) $\sigma_Z = 7.0$ mm (ATF2 bunch length) [16].

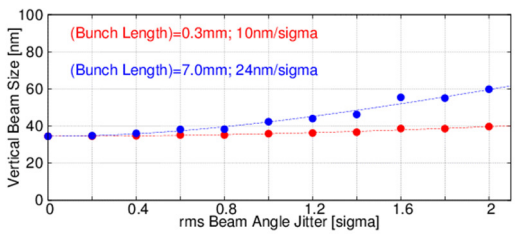

Figure 11: The IP angle jitter dependence of ATF2 beamline by the dipole cavities at $N = 1 \times 10^9$.

Table 3: Comparison of the Sensitivities of Intensity Dependence by IP Angle Jitter for ATF2/ILC

	ATF2	ILC	ILC/ATF2
Energy $(1/E)$	1.3 GeV	250 GeV	0.0052
N	1×10^9	2×10^{10}	20
σ_z	7 mm	0.3 mm	0.4
$\Sigma\beta_y$	58350	310584 m	5.32
Total			**0.22**

The ATF2 tuning procedures is also same to ILC. The vertical beam size was focused to less than 41 nm at the bunch population of 0.7×10^9 in ATF2 virtual IP. The achieved beam size is close to the ATF2 target value of 37 nm. The bunch population of ATF2 is much smaller than ILC. The reason why the bunch population of ATF2 is smaller than ILC is strong intensity dependence of beam size at the virtual IP. The candidate of the intensity dependence source is the IP angle jitter via wakefield. This is expected to be strong effect at ATF2, but will be insignificant for ILC. Therefore, it is very important for ILC to identify the mechanism of the ATF2 intensity dependence. The comparative study of the intensity dependence will be planned in 2016 autumn beam operation.

ACKNOWLEDGEMENT

Author would like to thank to all of group member of ATF international collaboration, especially for the ATF2 beam tuning group, and M. Yamauchi, S. Yamaguchi, S. Michizono and A. Yamamoto for their invaluable support of ATF2 project.

REFERENCES

[1] ATF2 proposal, KEK-Report 2005- 2 (2005).
[2] G. White *et al.*, Phys. Rev. Lett. **112** (2014) 034802.
[3] K. Kubo, Proc. of the IPAC'14 (2014) WEZA01.
[4] S. Kuroda, "ATF2 for final focus test beam for future linear colliders", Proc. of the ICHEP2014 (2014).
[5] ILC Global Design Effort, "ILC Technical Design Report", http://www.linearcollider.org/ILC/Publications/Technical-Design-Report (2013).
[6] K. Kubo *et al.*, Phys. Rev. Lett. **88** (2002) 194801.
[7] Y. Honda *et al.*, Phys. Rev. Lett. **92** (2004) 054802.
[8] P. Raimondi and A. Seryi, Phys. Rev. Lett., **86** (2001) 3779.
[9] T. Shintake, Nucl. Instrum. Meth., **A311** (1992) 455.
[10] V. Balakin *et al.*, Phys. Rev. Lett., **74** (1995) 2479.
[11] T. Suehara *et al.*, Nucl. Instrum. Meth., **A616** (2010) 1.
[12] T. Okugi *et al.*, Phys. Rev. ST-AB **17** (2014) 023501.
[13] N. Kraljevic *et al.*, Proc. of the IPAC'16 (2016) THPOR035.
[14] T. Okugi *et al.*, Proc. of the 13th PASJ (2016) MOOL04.
[15] J. Snuverink *et al.*, Phys. Rev. A. and B. **19** (2016) 091002.
[16] Simulated by A. Lyapin with GdfidL code (running on a cluster at RHUL), The wake potentials of ATF2 are summarized in http://atf.kek.jp/twiki/bin/view/ATF/Atf2Wakes .
[17] SAD is a computer program for accelerator design, http://acc-physics.kek.jp/SAD/ .

ISBN 978-3-95450-169-4